Analytical Methods

ROYAL SOCIETY OF CHEMISTRY

PAPER

View Article Online
View Journal

Cite this: DOI: 10.1039/d5ay02043c

Identifying small molecule impurities in electrospun poly(vinyl alcohol) nanofibres using ultra-selective NMR

Robert Evans, *[a] W. Joseph A. Homer,[b] Alice Millbank, [c] Bridget Tang, [c] Hana Ali, [a] Maxim Lisnenko, [d] Eva K. Kostakova,[d] Jan Valtera,[e] Vera Jencova, [d] Ralph W. Adams, [f] Paul D. Topham [c] and Eirini Theodosiou [bc]

Electrospinning is a widely employed manufacturing platform for preparing polymers for tissue engineering applications, producing structures that closely mimic the extracellular matrix. However, electrospinning is not benign, with high temperatures, pressures and voltages applied to the polymers throughout the process. Small molecule impurities have been detected using nuclear magnetic resonance (NMR) spectroscopy of electrospun poly(vinyl alcohol) materials. Different electrospinning techniques produce different impurities: DC needle electrospinning produces no observable impurities in the final sample, while both DC needleless and AC electrospinning produce a range of impurities. However, sample spectra feature both broad polymeric peaks and mixtures of the small molecule impurities. With most conventional NMR techniques, interpreting such spectra remains a major challenge. The use of ultra-selective magnetic resonance techniques, based on the GEMSTONE pulse sequence, allows for impurity peaks to be isolated, correlated to other signals in the spectrum, and for the structures of the chemicals responsible to be determined. Linear alkyl chains, differing in chain length, were identified in samples produced by DC needleless electrospinning. AC electrospinning produced small molecules with isopropyl groups, differing in molecular weight but not in structure, suggesting dimers, oligomers, or condensation products. For the set of samples measured, there was no apparent cytotoxic effect from the impurities. With a growing range of polymers processed by electrospinning, identification of small molecule impurities, and their effects on biomedical applications, will be increasingly important.

Received 8th December 2025
Accepted 20th March 2026

DOI: 10.1039/d5ay02043c

rsc.li/methods

Introduction

Electrospinning is a widely employed manufacturing platform for scaffolds, such as in tissue engineering, because it can produce structures with controllable morphology and porosity from a wide array of natural and synthetic polymers. With a successful experimental history dating back decades, if not centuries,[1,2] there is a wide range of examples, applications and innovations.[3–7] In electrospinning experiments, electrical forces, whether from direct (DC electrospinning[8,9]) or alternating (AC electrospinning[10,11]) currents, transform polymer solutions into a fibrous material. The material is then driven onto a collector, resulting in the formation of a fine liquid jet with a diameter in the micro-to nanometre range. The process is 'green', fast, scalable, and can be highly cost-effective.[8] The nanofibrous constructs, often taking the form of thin mats, have high surface area-to-volume ratio and closely resemble the architecture of the extracellular matrix, making them ideal surfaces for cell proliferation, moisture retention, and drug delivery.[3,12]

Poly(vinyl alcohol) (PVA) is currently one of the most promising materials for electrospinning into tissue engineering and wound management applications.[11,13,14] This synthetic, hydrophilic and water-soluble polymer is FDA-approved for food packaging and biomedical applications due to its biocompatibility, biodegradability and non-toxic nature.[15,16] It is commonly produced *via* hydrolysis or transesterification of poly(vinyl acetate),[17] as depicted in Fig. 1.

The properties of the final polymer material depend not only on the degree of polymerisation but also the degree of hydrolysis, the percentage conversion of acetate groups into hydroxyls, which can range from 85–90% up to 99% and higher. One of the major drawbacks of PVA, preventing its use in cell-

[a]*Chemical Engineering and Applied Chemistry, Aston University, Birmingham B4 7ET, UK. E-mail: robert.evans@manchester.ac.uk*

[b]*Engineering for Health Research Centre, College of Engineering and Physical Sciences, Aston University, Birmingham B4 7ET, UK*

[c]*Aston Institute for Membrane Excellence, Aston University, Birmingham, B4 7ET, UK*

[d]*Department of Chemistry, Faculty of Science, Humanities and Education, Technical University of Liberec, Liberec, Czech Republic*

[e]*Department of Textile Machine Design, Faculty of Mechanical Engineering, Technical University of Liberec, Liberec, Czech Republic*

[f]*Department of Chemistry, The University of Manchester, Oxford Road, Manchester M13 9PL, UK*

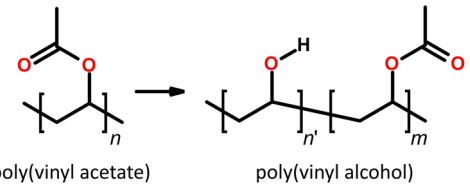

Fig. 1 Synthesis of poly(vinyl alcohol) *via* hydrolysis of poly(vinyl acetate).

friendly aqueous environments, is its instability in water. Several strategies have been proposed to stabilize PVA nanofibres, including heating, exposure to cross-linking agents and irradiation.[18,19] Of these, heat treatment can achieve very stable fibres in the absence of toxic chemicals, whilst simultaneously sterilizing them for subsequent contact with cells.[13]

Electrospinning processes force the polymer to experience high temperatures, high pressures and high voltages. Changes in the polymer structure and properties upon electrospinning are well reported.[20] Differences in scaffold morphology are observed when different electrospinning methods, such as direct current (DC) needle and needleless, and alternating current (AC), are used. These can be observed in electron microscopy images. Fig. 2 depicts electrospun mats, similar to those created in this study (see materials and methods – electrospinning), and illustrates morphological changes that can result from different electrospinning techniques, when applied to poly(vinyl alcohol). DC needle electrospinning produces fibres with the smallest average diameters, followed by DC needleless Nanospider™ and finally AC spinning. Furthermore, the fibres from the two DC methods appear more densely packed than those from the AC one. It is important to note that different operating conditions for the samples depicted here, detailed in the methods and materials section, were employed to optimise the fibre morphology for each technique.

What is less well understood is whether chemical changes also occur. In the polyamides, nylon-6 and nylon-12, differences in the chain conformation have been observed after electrospinning.[21] Kim and Lee reported changes in the intrinsic viscosities of poly(ethylene terephthalate) and poly(ethylene naphthalate) samples after electrospinning.[22] It was suggested that this observation was due to decreases in the molecular weights of the polymers involved, as the polyesters used were susceptible to degradation of the ester under similar conditions. However, to the best of our knowledge, there have been no previous studies of small molecule impurities occurring in electrospun polymer materials. Such small molecule impurities will not be visible to all analytical techniques, particularly those commonly used for characterising polymers. Gel permeation chromatography (GPC) is able to provide information on the polymer chain lengths, but is not suited for the study of small molecules. Dynamic scanning calorimetry (DSC) can be used to identify differences in structure and packing, such as differences in crystallinity between samples. Any infrared-based spectroscopic method will only identify functional groups, almost completely independent of the size of the molecules they belong to.

Nuclear magnetic resonance (NMR) spectroscopy, however, is very well-suited to studying this problem. This near-ubiquitous analytical chemistry technique is capable of resolving molecular information and can provide detailed information about the structure of molecules in solution, through 2-dimensional techniques such as correlated spectroscopy (COSY). One common hindrance to successful analysis of NMR spectra is the case where peaks overlap. Broad signals, such as those produced by the polymers in the samples studied here, can easily span several parts per million and swamp the signals of other species in the sample, particularly those from minor components or smaller molecules. A number of NMR techniques have been developed to overcome this common problem. These can be classified according to whether they filter the spectrum, simplify the spectrum, or select only a particular subset of signals.

Spectral filtration can be carried out according to a number of different criteria, including both complexity of spin system[23,24] and physical parameters, such as mobility and size.[25,26] Diffusion-weighting of the spectra will remove peaks belonging to the smallest species, as they typically move faster and their signals attenuate more quickly in a pulsed field gradient NMR experiment.[27] The opposite effect can be achieved using perfect-echo-based sequences such as PROJECT.[26] These

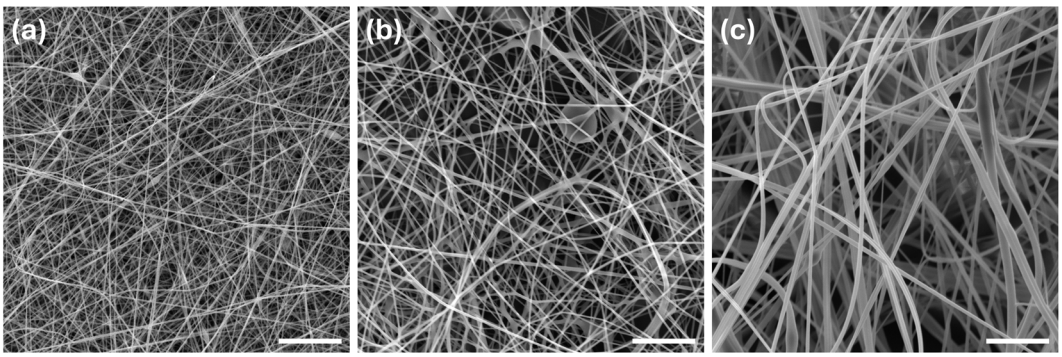

Fig. 2 SEM images of nanofibrous PVA scaffolds produced using: (a) DC needle, (b) DC needleless Nanospider™ and (c) AC electrospinning scale bar: 10 μm.

filter according to the relaxation times of the species present, with the smaller relaxation time constants of larger species contributing to more efficient filtration from the final spectrum.

Simplification of the spectrum can be achieved by decoupling. This can be hetero- or homo-nuclear in nature. In the former, couplings between different nuclei of different types are removed, as in many two-dimensional experiments, as well as the DISPEL and ODYSSEUS experiments.[27,28] These can be useful for identifying minor impurities hidden amongst a low scrub of satellite peaks. Broadband homonuclear decoupling, or 'pure shift' NMR, is a relatively recent addition to the NMR toolkit.[29,30] This set of experiments reduces all the characteristic multiplets in a standard ^{1}H NMR spectrum to a single peak for each chemical site. For the loss of some signal-to-noise ratio, there is a significant gain in resolution. The first generation of pure-shift experiments used the Zangger–Sterk pulse sequence element, a selective radiofrequency (RF) pulse applied simultaneously with a weak magnetic field gradient.[31] Selective RF pulses of all shapes have a long history in NMR spectroscopy.[32] Such pulses are typically longer in duration and at a lower power, acting over a narrower range of spectral frequencies than those used in non-selective experiments. The longer the pulse, the more selective, with a narrower band of frequencies affected. The recent PSYCHE series of pure shift NMR experiments have replaced the selective pulses with frequency-swept pulses based on CHIRPs.[33,34] This substitution has made pure shift techniques significantly more robust, and free from artefacts, to warrant routine use.

Pushing simplification to its extreme, it is also possible to select only a particular set of signals of interest. Again, this can be achieved by selective pulses, shaped pulses applied for a long duration at low power. However, many common shaped pulses would need to be unfeasibly long in order to be highly selective. An additional complication arises when peaks overlap, as it becomes impossible to excite one without affecting nearby peaks. Again, a switch to CHIRP pulses reaps dividends. The ultra-selective GEMSTONE pulse sequence applies a pair of long, adiabatic pulses synchronously with weak magnetic field gradients.[35] This effectively produces a single-shot chemical shift selective filter.[36] Different resonance offsets experience the RF pulses at different times and at different positions while the pulse is being applied. Only spins with their chemical shift exactly on resonance end up with the same phase throughout the sample and only these spins remain in the final spectrum. Those signals that are off-resonance develop a position-dependent phase and average to zero. Hence, distinct multiplets and coupled spin systems can be retrieved from even very highly crowded spectra.[37]

In this work, we demonstrate that the previously observed physical and morphological changes in non-woven electrospun poly(vinyl alcohol) materials are also accompanied by chemical changes. Small molecule impurities embedded within, with chemical structures depending on the method of electrospinning. It is only possible to successfully identify these impurities with the use of complementary, advanced proton NMR techniques, particularly ultra-selective techniques that simplify the spectra or select only a subset within. The NMR data acquired provides important information about the structures of the impurities present, sufficient to differentiate between the different samples.

Methods and materials

Electrospinning

PVA 'Mowiol 28–99' (99% hydrolysed, 145 000 Mw; Sigma-Aldrich, Merck KGaA, Darmstadt, Germany) was dissolved at 8% (w/w) in either de-ionised water (for AC electrospinning) or 9 : 1 (w/w) deionised water: ethanol solvent ratio (for DC electrospinning) and heated at 90 °C for 4 h while stirring intermittently. After fully dissolving the PVA, solutions were allowed to cool to room temperature and left to settle overnight before final stirring to ensure homogeneity.

DC needle electrospinning was carried out using an in-house set-up. Solutions were loaded into a disposable polypropylene syringe fitted with a 22-gauge blunt-tipped Metcal Blue Straight Dispensing Needle (RS, UK), and mounted onto a syringe pump (NE-300, New Era Pump Systems Inc., USA). Electrospinning was performed at 9 kV with a 15 cm tip-to-collector distance, depositing fibres onto non-stick baking paper. The flow rate was adjusted between 0.03 and 0.10 mL h^{-1} to stabilise the Taylor cone and ensure consistent fibre formation. Electrospinning continued for 16 h to produce mats of sufficient thickness. Climate control was not possible in this setup, but humidity and temperature were recorded using a humidity meter (Fisherbrand Traceable Humidity/Temperature Meter/Recorder, Fisher Scientific UK Ltd, Loughborough, UK) with all utilised samples being spun within the ranges of 25–30 °C and 48–57% RH.

DC needleless electrospun samples were produced using static wire spinning electrode (Nanospider™, Elmarco NS 1S500U; Liberec, Czech Republic), with a 50 kV voltage differential (+40 kV and −10 kV) and an electrode separation distance of 16 cm. Spinning solution was applied to the positively charged electrode (wire with diameter 0.25 mm) by traversing cartridge with a capillary die diameter of 0.7 mm. Climate parameters were fixed at 22 °C and 30% RH by a precision air conditioning unit (NS AC150, Elmarco; Liberec, Czech Republic).

AC electrospinning employed a rod-like spinning electrode with emitter diameter of 22 mm.[38] The electrically inactive drum had a diameter of 30 cm, rotated at 10 rpm and the emitter-drum surface distance was 17 cm. An effective voltage of 35 kV with a 30 Hz sinusoidal waveform was applied to the emitter using a high voltage supply. Spunbond nonwoven fabric (30 g m^{-2}) was used as collector material in both the DC needleless (Nanospider™) and the AC equipment.

FT-IR characterisation

Fourier transform infrared spectroscopy (FT-IR) was conducted with a Frontier Spectrometer (PerkinElmer Ltd, Waltham, MA, USA) combined with an attenuated total reflectance (ATR) accessory (GladiATR; Pike Technologies, Madison, WI, USA).

Each scan was performed from 4000 cm^{-1} to 700 cm^{-1} with a resolution of 4 cm^{-1} for a total of 16 scans per measurement.

NMR spectroscopy

Initial NMR experiments were carried out on a 300 MHz Bruker Avance spectrometer, using a 5 mm BBO probe equipped with a *z* gradient coil producing a maximum gradient strength of 0.55 T m^{-1}. All NMR experiments were performed at a regulated 298 K. ^{1}H NMR experiments consisting of 4 scans, 1 dummy scan and an acquisition time of 11 seconds were acquired using a simple pulse-acquire sequence with a 30° tip angle.

COSY experiments were acquired with a gradient-enhanced double quantum filtered COSY experiment.[39] Experimental parameters depended on both the sample and the final spectrum resolution and signal intensity being sought. Typical experimental parameters were 128 or 256 increments in the indirect dimension and an acquisition time for each FID of *ca.* 2 seconds.

Diffusion NMR experiments were performed with a double stimulated echo bipolar pulse pair sequence, with additional balancing gradients added to reduce the effect of the gradient pulses on the lock. This sequence was chosen to reduce the possible effects of convection.[40] The gradient encoding time for all experiments was 1 ms and all gradients were half-sine in shape. For each gradient amplitude, 128 transients of 16 384 complex datapoints were acquired for a total experimental time of *ca.* 1 hour and 45 minutes. The diffusion delay time, Δ, was set to 0.1 s, sufficient to obtain *ca.* 80% attenuation of signals arising from small molecules in the samples. Diffusion coefficients and DOSY spectra were subsequently determined and processed using the DOSY Toolbox software package.[41] Reference deconvolution was used and produced separated methyl peaks in the proton dimension.

GEMSTONE[35] and PSYCHE pure shift[42] experiments were carried out on a 500 MHz Bruker NEO. The modified GEMSTONE sequence detailed in SI SI.1 was used. Experiments consisted of 8 transients with 1 dummy scan. The WURST pulses had bandwidths of 9 kHz, durations of 200 ms, and were applied alongside synchronous weak gradients corresponding to 1% of the maximum gradient strength of the probe. The selective 180 pulse was an RSnob pulse with 25 Hz bandwidth, flanked by gradients 15% of the maximum of the probe. The GEMSTONE-TOCSY[37] experiments used a GEMSTONE experiment, with parameters described above, coupled to a one-dimensional TOCSY sequence, using a DIPSI2 spinlock. 256 Transients and 1 dummy scan were acquired for each target frequency. The PSYCHE experiments consisted of 60 increments, each of 8 transients, reconstructed using a chunking algorithm to give a 1D 'pure shift' FID. The SALTIRE pulse had a bandwidth of 10 kHz, a duration of 30 ms, and was applied alongside a synchronous weak gradient corresponding to 2% of the maximum gradient strength of the probe.

Cell culture and cytotoxicity

Bovine mesenchymal stem cells (bMSCs) at passage 5 were cultured in α-MEM supplemented with 10% (v/v) foetal bovine serum (FBS), 1% (v/v) penicillin–streptomycin, 1 ng mL^{-1} basic fibroblast growth factor (bFGF), and 2 mM L-glutamine, as described by Dagès *et al.*[43] Cells were maintained at 37 °C with 5% CO_2. A direct contact cytotoxicity assay was used to assess the effects of electrospun mats on bMSC viability through physical interaction. Prior to cytotoxicity experiments, the electrospun mats were carefully peeled from the collector material and heat-treated inside loosely folded foil pouches in a Fan Assisted High Temperature Oven 80 HT (SciQuip Ltd, UK) at 180 °C for 4 h to ensure complete water evaporation and structural stabilisation. Discs were then punched from the mats using a puncture tool of known radius and transferred to sterile petri dishes. UV sterilisation was performed for 24 hours prior to cell seeding experiments.

Cells were seeded into 96-well plates at a density of 5×10^3 cells cm^{-2} and allowed to adhere and proliferate until a monolayer was established. Electrospun mats were then placed directly onto the cell layer, followed by the addition of fresh culture medium. Culture medium was used as blank, cells cultured in the absence of electrospun mats were the negative control and cells treated with 70% (v/v) ethanol to induce a cytotoxic response served as the positive control.

After 24 hours of incubation, mats were gently removed using a sterile disposable pipette attached to a vacuum handle, ensuring minimal disturbance to the underlying cell layer. Cell viability was quantified using the PrestoBlue™ assay (10% (v/v) PrestoBlue in culture medium). This assay is based on the reduction of resazurin to resorufin by metabolically active cells, producing a fluorescent signal proportional to cell viability. Plates were incubated with the assay reagent for 30 min at 37 °C in 5% CO_2. Fluorescence was then measured at 544 nm excitation and 590 nm emission using a FLUOstar Omega plate reader (BMG LABTECH, Germany) with background fluorescence subtracted using the blank control. Mats were classified as non-cytotoxic if the Relative Fluorescence Units (RFU) were comparable to the negative control (≥70% viability). A decrease in RFU below this threshold was considered indicative of potential cytotoxicity.

Results and discussion

Sample characterisation using FT-IR

FT-IR is used routinely to identify chemical changes that occur during electrospinning. Fig. 3 compares IR spectra of three samples produced *via* the three different electrospinning methods. The overall chemical identity of the samples is highly consistent. There is some indication of small differences in the spectra around the 980 cm^{-1} region, which could be attributed to carbon–carbon double bonds, and around the 2900–3000 cm^{-1} which has been associated with CH bonds in methyl, methylene and methine groups. There is also a slight increase in the band at 1144 cm^{-1}, linked to crystallinity, suggesting that fibres produced by the Nanospider™ and AC spinning possess a higher degree of crystallinity than those produced by needle electrospinning.

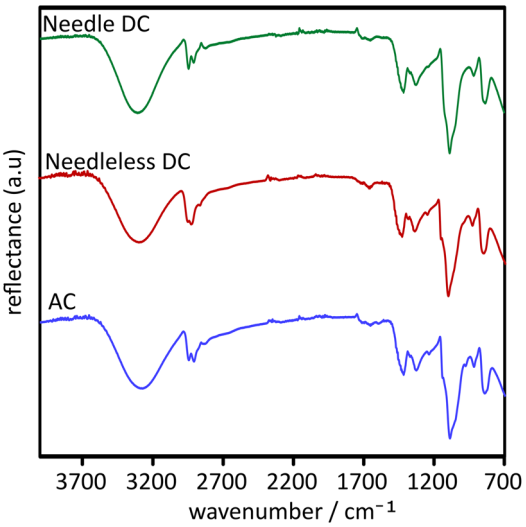

Fig. 3 FT-IR spectra of samples of 99% hydrolysed PVA produced by three methods of electrospinning: DC needle (green), DC needleless (Nanospider™) (red) and AC (blue).

Sample characterisation using NMR

All PVA samples studied were at least partially soluble in D_2O. Fig. 4 depicts proton NMR spectra of three different PVA samples in solution. Only the regions between −1.0 and 5.5 ppm are shown, there were no signals at higher chemical shifts than the water solvent. An expansion, showing the region between 0.4 and 2.4 ppm, is also included. Each sample has undergone a different electrospinning procedure: the top spectra depict sample produced by AC electrospinning, middle spectra depict sample produced by DC needleless electrospinning (Nanospider™), and bottom spectra depict sample produced by DC needle electrospinning.

In all three spectra, the broad peaks from the PVA backbone are not only present but identical: the only differences arise from smaller impurity signals. DC needle electrospinning appears to produce no impurities in the final sample, whereas both DC needleless and AC electrospun samples have additional peaks at *ca.* 0.9 ppm and between 3.4 and 3.8 ppm. These are sharper than the polymer peaks and likely correspond to methyl groups, short alkyl chains and polar substituents.

The enlarged spectrum of the region between 0.3 and 2.3 ppm, focusing on the methyl and methylene groups, indicates that the methyl peaks in the DC needleless electrospun sample form a triplet, while there are several peaks present in this region of the AC electrospun sample. These results are supported by Fig. SI.2.1 in SI SI.2, which depicts the chemical shifts between 3.3 to 4.1 ppm. These methyl peaks are not present in PVA solutions before electrospinning, as discussed in SI SI.3.

Two-dimensional NMR techniques, such as COSY, are highly useful in resolving coupling patterns and connections within a molecule. As observed in Fig. 5, the PVA peaks have large footprints in both dimensions of the COSY spectrum. Data from both spectrometers used in this work are presented in Fig. 5. It would normally be expected that the spectra acquired at 500 MHz would have improved resolution, but the PVA peaks are so broad that there is little improvement upon moving to a higher

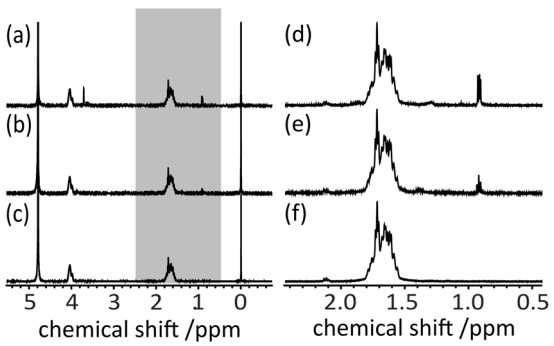

Fig. 4 1D ^{1}H NMR spectra of three electrospun PVA samples, dissolved in D_2O. Spectra (a), (b) and (c) depict whole region of chemical shifts, while spectra (d), (e) and (f) depict chemical shifts between 0.4 and 2.4 ppm. Spectra (a) and (d), sample prepared by AC electrospinning, spectra (b) and (e), sample prepared by DC needleless electrospinning (Nanospider™) and spectra (c) and (f), sample prepared by DC needle electrospinning. Spectra of chemical shifts between 3.2 and 4.2 ppm can be found in SI SI.2.

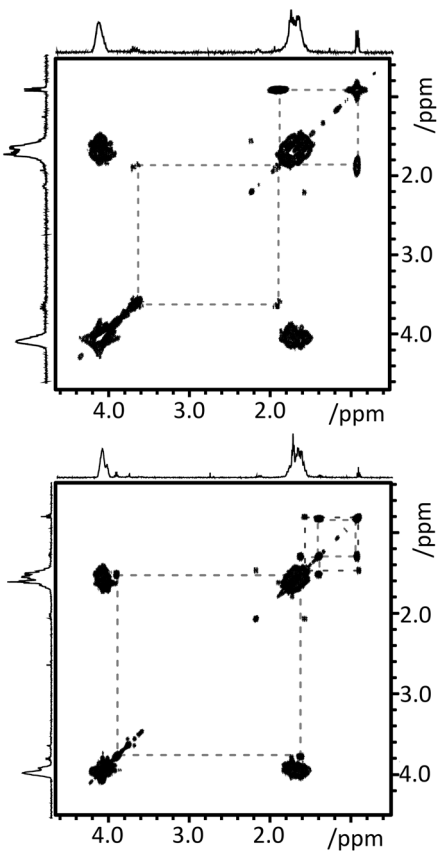

Fig. 5 COSY spectra of (top) AC electrospun PVA, acquired on a 300 MHz spectrometer, and (bottom) DC needleless Nanospider™ electrospun PVA samples, acquired on a 500 MHz spectrometer. Dashed lines have been added to highlight correlations between signals.

magnetic field strength. The broad PVA peaks overlap with several smaller peaks which are present due to impurity molecules in the samples. These impurities are visible as well-resolved cross-peaks in the COSY spectra. The methyl signals in the AC electrospun sample (Fig. 5(a)) overlap enough, particularly in the indirect dimension, for them to only appear as one peak. These signals couple to signals that are not only close together in frequency but also swamped by the methyl peaks of the polymer. This hinders the analysis of the AC electrospun sample. There is better resolution in the Nanospider™ sample (Fig. 5(b)). Both a major and a minor impurity are observed, each with a distinctive triplet methyl signal and resolved cross peaks. These data indicate that the impurities are mostly unbranched butyl chains, with a small population of propyl chains, both with polar groups, likely hydroxyls, at one end.

With both large polymers and small molecules present in the samples, PROJECT-based T_2 filtration experiments were carried out. These experiments should remove the polymer peaks leaving only the impurity peaks in the final spectrum. Disappointingly, there were three drawbacks to this relatively conventional approach. First, the filter is not targeted and signals from every small species present, including *e.g.* common solvents, remain. Second, all signals are reduced in intensity, with a corresponding reduction in the quality of the spectrum, decreasing the resolution of the remaining signals. Third, while it is possible to prepend experiments with a PROJECT filter, *e.g.* a PROJECT-COSY, this further increases the duration of the NMR experiment leading to a degraded final spectrum and no additional gain in information. While ultimately fruitless, an overview of these studies, and their experimental details, can be found in the SI SI.4.

The GEMSTONE family of ultra-selective NMR techniques offers a complementary approach. Using GEMSTONE, it is possible to select one peak out of a crowded, overlapping spectrum. Fig. 6 summarises a series of GEMSTONE and GEMSTONE-based experiments performed on the AC electrospun PVA sample. The proton spectrum from Fig. 3 is reproduced, as are the methyl peaks at *ca.* 0.9 ppm as Fig. 6(a) in the inset. These appear as a doublet-of-doublets multiplet. The GEMSTONE experiment is selective enough for each constituent doublet to be revealed. Small artefacts can be observed in the presented data, corresponding to 'ghost' peaks of the other doublet. These were present in all GEMSTONE experiments but could be significantly mitigated by alternating the sign of the applied field gradient in subsequent scans of the experiment. This modification to the GEMSTONE sequence is described in SI SI.1. The GEMSTONE experiments indicate that the cluster of additional peaks at *ca.* 0.9 ppm in the AC electrospun sample can be successfully resolved into two doublets. These doublets correspond to distinct chemical species. The sum of the two 1D GEMSTONE experiments replicates the original proton experiment, confirming the analysis. The GEMSTONE-TOCSY experiment goes one step further, confirming the coupling information contained within the COSY spectrum of Fig. 5(a). The methyl peaks couple with a broad multiplet at 1.8 ppm, which would otherwise be swamped by the polymer signals. The individual GEMSTONE-TOCSY experiments, presented here as the sum of the spectra, can be found depicted in Fig. SI.5.1 in SI SI.5.

Diffusion-ordered NMR spectroscopy, DOSY, produces spectra with species ordered along the vertical axis according to the speed with which they move through solution. With two species identified in AC electrospun PVA sample through use of COSY and GEMSTONE, diffusion NMR data, presented as a DOSY spectrum in Fig. 7, illustrates how it is possible to differentiate between the two species present in these samples. Fig. 7 depicts only the region containing the isolated methyl peaks, between −0.3 and 1.3 ppm. Alongside the GEMSTONE and DOSY experiments, a PSYCHE pure-shift spectrum was acquired, included as an insert in Fig. 7.

Fig. 7 confirms that there are two separate species contributing to the methyl multiplet. With judicious use of reference deconvolution using the TMS peak, the lineshapes of the sample peaks can be rendered narrow enough for them to be resolved in a DOSY spectrum. This allows for the two species to be separated in both the chemical shift and the diffusion dimensions. Each methyl peak splits into a doublet, indicating a branched isopropyl motif and consistent with both GEMSTONE and PSYCHE experiments: both experiments indicated a pair of species present in this sample. The two species are not part of the polymer network, moving as small molecules when dissolved, but they do have different sizes.

A second DOSY spectrum of the AC electrospun PVA sample, spanning all relevant chemical shifts, can be found in SI SI.6 as Fig. SI.6.1. In this additional figure, line broadening of 2 Hz has been added to broaden all signals and simplify the resulting DOSY spectrum. As expected, the PVA signals move very slowly in solution. These signals are highlighted with dark blue shading. As the COSY spectra in Fig. 4 indicates, most of the impurity peaks overlap strongly with the PVA signals. The overlap of these signals renders the diffusion coefficients acquired in this region, indicated by red shading in the figure, highly unreliable. Finally, the region corresponding to Fig. 7 has also been highlighted. Here, the impurity signals, identified in Fig. 4, do not overlap with the polymer peaks and a good quality DOSY spectrum can be obtained.

While the two main impurities in the DC electrospun sample differed in terms of the lengths of the unbranched alkyl chain, the compounds identified in the AC electrospun sample both feature isopropyl groups connected to a further methylene group. The COSY spectrum (Fig. 3(a)) shows very little difference in their chemical shifts, suggesting that these are very similarly structured compounds, potentially even condensates or dimers. Fig. 8 summarises the key details of the NMR study, providing likely identities for the impurities observed.

Cytotoxicity of electrospun mats

The effect of the small molecule impurities introduced to the PVA non-woven mats from the different electrospinning methods was further investigated in terms of their biological performance. For many of the planned applications, such as wound healing, the materials will be in direct contact with cells.

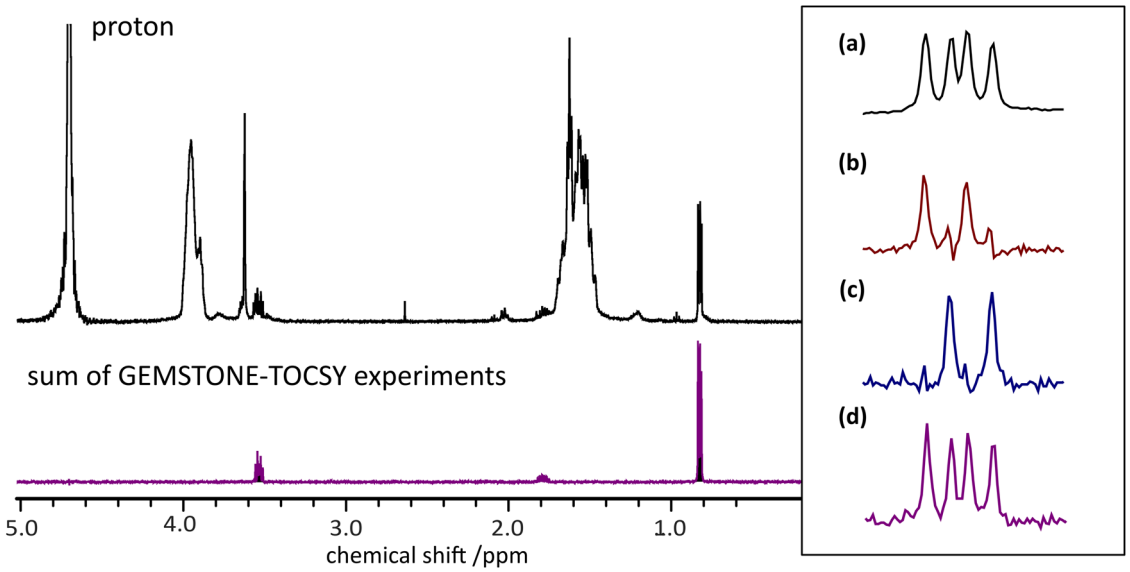

Fig. 6 Summary of GEMSTONE-related NMR spectra of the AC electrospun PVA sample. Top major spectrum reproduces the proton spectrum of the AC electrospun sample from Fig. 4. The insert focuses on methyl peaks at 0.8 ppm. (a) shows the proton spectrum. (b) and (c) are GEMSTONE spectra focused on the left-hand and right-hand methyl peaks respectively. (d) Is the sum of the two GEMSTONE experiments ((b) + (c)), reproducing the proton spectrum. The bottom major spectrum is the sum of two GEMSTONE-TOCSY experiments, based on experiments (b) and (c), as well as their sum (d).

Therefore, it is crucial to assess their potential cytotoxicity.[44,45] Fig. 9 shows the presence of viable mesenchymal stem cells following 24 h of direct contact with mats produced with DC needle, DC needleless and AC electrospinning.

The fluorescence data reveals little difference between the three electrospinning methods, with all three measurements comparable to the negative control. This clearly indicates that any impurities present do not kill the cells and, therefore, these PVA mats can still be considered as suitable for tissue engineering applications. These findings align well with previously reported cytotoxicity data for PVA-based biomaterials. For instance, Díez *et al.* observed minimal cytotoxic effects when human fibroblasts were cultured in direct contact with DC needle-electrospun PVA mats for 24 and 72 hours.[44] Similarly, Teixeira *et al.* demonstrated that PVA-based scaffolds can support a wide range of cell types relevant to tissue engineering applications, including endothelial cells, primary chondrocytes, and human mesenchymal stem cells.[46]

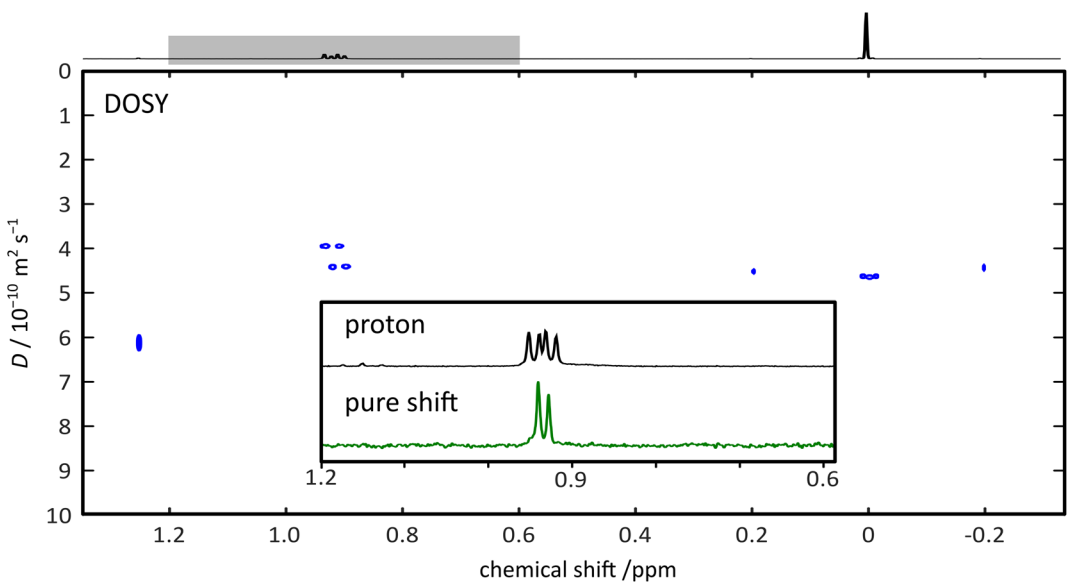

Fig. 7 Combined DOSY and pure shift NMR spectra of the AC electrospun PVA sample. Insert highlights peaks at *ca.* 0.9 ppm, contrasting the original proton spectrum (black insert) with a PSYCHE pure shift spectrum (green insert).

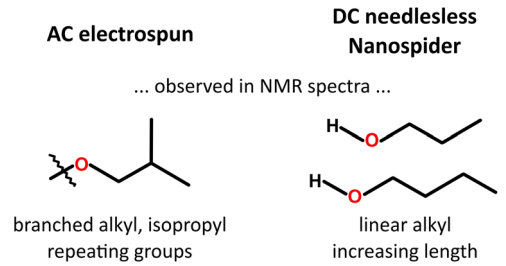

Fig. 8 Summary of possible identities for small molecule impurities observed in PVA fibres, as detected by NMR spectroscopy.

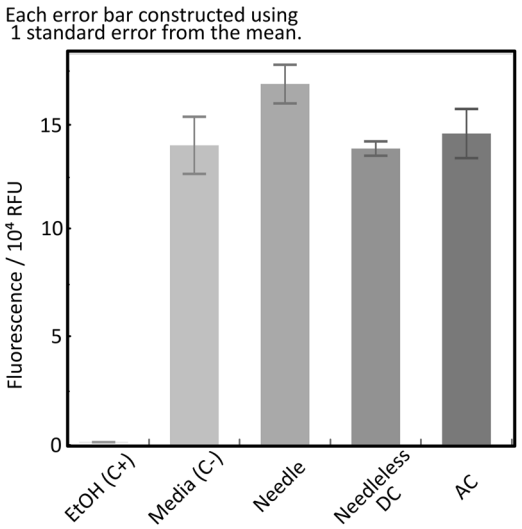

Fig. 9 Cytotoxicity data, expressed as Relative Fluorescence Units (RFU), of bovine mesenchymal stem cells following direct contact with the electrospun mats for 24 h. C(+) refers to the cytotoxic response in the presence of 70% (v/v) ethanol, and C(−) corresponds to cell growth in the absence of polymer mats. Each error bar is constructed using 1 standard error from the mean.

Nevertheless, additional characterisation (particularly analyses of cell viability, morphology, and proliferation over extended culture periods, and involving other relevant cell types such as dermal fibroblasts) would be required before firmer conclusions can be drawn regarding the influence of different electrospinning techniques on the functionality of the mats as tissue-engineering devices.

Conclusions

Electrospun polymers offer great potential as nanofibrous supports in a wide range of applications, most notably in healthcare settings. Much of the research in this field concerns their synthesis, followed by characterisation of physical properties and macroscopic behaviour. However, the manufacturing process involves high temperatures, high pressures and high voltages. Different processing conditions have been shown to induce different structures on the nanometre and the micrometre scale.

In this work, previously observed morphological changes in the polymer fibres are shown to be accompanied by chemical changes. To the best of our knowledge, this is the first time that small molecule impurities have been detected within the polymer scaffolds. These impurities are not observed by traditional polymer analyses. Standard NMR techniques struggle due to the overlap of signals. It requires recently published ultra-selective NMR techniques to successfully isolate and identify the impurities, obtaining enough information to deduce possible chemical structures for the impurities.

Several key points follow. First, the conditions of electrospinning are not benign and can induce chemical changes in the processed polymers, producing small molecule impurities. Second, different electrospinning methods produce both different amounts and different types of small molecule impurities. DC needle electrospinning produced no impurities. DC needleless Nanospider™ electrospinning produced linear molecules, likely alcohols, with different length alkyl chains. AC electrospinning produced branched chains, again likely alcohols, with a distinctive iso-propyl motif identified. Molecules of similar structures yet distinctly different molecular weights were identified. An open question remains how the different structures are produced by the different processing methods. In particular, the branched chain observed in the AC electrospinning does not feature in the original polymer. Some rearrangement of the carbon–carbon bonds is required.

Care must be taken not to over-interpret these results. The synthesis of PVA from PVAc is a base-catalysed hydrolysis of ester groups, typically using a methanolic solution. Side products include sodium acetate and residual impurities include NaOH and methanol,[47] some of which can be observed in the initial PVA feedstock, as illustrated in Fig. SI.3.1 and SI.3.2. However, these molecules are not present in any of the electrospun materials, as indicated by both NMR and IR spectroscopy. Indeed, practically no impurities can be observed in the AC electrospun polymer (Fig. 4(c) and (f)), evidence that any small molecules present at the start of the electrospinning process neither takes part in any chemistry during processing nor remains in the sample. It is common practice to add co-solutes, such as ethanol, to the feedstock in the DC electrospinning experiments. It is readily confirmed, by 1D ^{1}H (Fig. 4) or by COSY NMR spectra (Fig. 5, but also see Fig. SI.3.3), that ethanol is not present in either sample. SI SI.3 presents both spectra and literature data to further illustrate these arguments. Finally, these are aqueous samples of the electrospun polymer materials and represent only the water-soluble fractions present. GPC, DSC and IR spectroscopy are all discussed earlier in the manuscript and may yet prove useful in understanding the chemical processes accompanying electrospinning, by giving information on *e.g.* polymer chain lengths and crystal structure before and after the process.

Finally, in the polymer system studied here, initial cytotoxicity experiments reveal that all three types of materials are cell-friendly, although the full impact of these small molecules on cell viability, proliferation and cellular metabolism needs to be determined in further studies. It would be expected that different polymers will degrade in different ways. The extreme

conditions induced by the process are likely to cause similar effects in other polymers used for electrospinning. These polymers could be simple, synthetic polymers, such as poly(ethylene oxide), polyesters, such as poly(caprolactone),[48] and even naturally occurring polymers, such as gelatin or hyaluronic acid.[49] Whether any of these break down upon electrospinning, and what impurities are then formed, remains to be seen. The presence of small molecule impurities may have significant implications in the final applications of these materials or at least necessitate additional purification steps.

Author contributions

RE – conceptualisation, investigation, methodology, resources, supervision, visualization writing – original draft preparation, reviewing, editing; WJAH – investigation, methodology, validation, reviewing, editing; AM – investigation, validation, formal analysis, reviewing, editing; BT – investigation, formal analysis; HA – investigation, formal analysis; ML – investigation, validation, reviewing, editing; EKK – funding acquisition, investigation, methodology, resources, supervision, reviewing, editing; JV – funding acquisition, investigation, methodology, resources, supervision, reviewing, editing; VJ – funding acquisition, investigation, methodology, resources, supervision, reviewing, editing; RA – investigation, methodology, resources, reviewing, editing; PDT – resources, reviewing, editing; ET – conceptualisation, investigation, resources, supervision, methodology, writing – original draft preparation, reviewing, editing.

Conflicts of interest

There are no conflicts to declare.

Data availability

All NMR data can be found at https://doi.org/10.17632/zmbgkdrbz3.2

Supplementary information (SI): modified GEMSTONE NMR pulse sequence, additional proton NMR spectra, summary of PROJECT NMR experiments, GEMSTONE-TOCSY experiments, additional details supporting Diffusion-Ordered Spectroscopy, and additional details on impurities within PVA. Ref. 50 has been cited in the SI. See DOI: https://doi.org/10.1039/d5ay02043c.

Acknowledgements

RE would like to thank Connect NMR UK (grant number EP/S035958/1) for a Training Mobility Grant and RA for training and support with installing the GEMSTONE pulse sequences. RA was supported by the Engineering and Physical Sciences Research Council (grant number EP/V007580/1). WJAH, ET and VJ acknowledge financial support from the Royal Society International Exchanges grant IES\R3\183098 and the Birmingham Orthopaedic Charity. AM acknowledges financial support from the Engineering and Physical Sciences Research Council (EPSRC) Doctoral Training Program, grant number EP/W524566/1. HA was funded by an Aston Institute of Materials Research Seedcorn Grant in Summer 2021. VJ, ML, EKK and JV acknowledge financial support from the Czech Health Research Council projects No. NV18-01-00332 and NV24-08-00073. The Aston Institute for Membrane Excellence (AIME) is funded by UKRI's Research England as part of their Expanding Excellence in England (E3) fund.

References

1 N. Tucker, J. J. Stanger, M. P. Staiger, H. Razzaq and K. Hofman, *J. Eng. Fibers Fabr.*, 2012, **7**, 64–73.
2 A. Keirouz, Z. Wang, V. S. Reddy, Z. K. Nagy, P. Vass, M. Buzgo, S. Ramakrishna and N. Radacsi, *Adv. Mater. Technol.*, 2023, **8**, 2201723.
3 G. Z. Tan and Y. Zhou, *Int. J. Polym. Mater. Polym. Biomater.*, 2019, **69**, 947–960.
4 J. Xue, T. Wu, Y. Dai and Y. Xia, *Chem. Rev.*, 2019, **119**, 5298–5415.
5 M. Rahmati, D. K. Mills, A. M. Urbanska, M. R. Saeb, J. R. Venugopal, S. Ramakrishna and M. Mozafari, *Prog. Mater. Sci.*, 2021, **117**, 100721–100759.
6 N. Angel, S. Li and L. Kong, *J. Future Foods*, 2024, **4**, 289–299.
7 J. Wu, F. Yu, M. Shao, T. Zhang, W. Lu, X. Chen, Y. Wang and Y. Guo, *ACS Appl. Bio Mater.*, 2024, **7**, 3556–3567.
8 S. A. H. Ravandi, A. Sadrjahani, A. Valipouri, F. Dabirian and F. K. Ko, *Text. Res. J.*, 2022, **92**, 5130–5145.
9 A. Blanquer, E. K. Kostakova, E. Filova, M. Lisnenko, A. Broz, J. Mullerova, V. Novotny, K. Havlickova, S. Jakubkova, S. Hauzerova and B. Heczkova, *Nanoscale*, 2024, **16**, 1924–1941.
10 O. Batka, J. Skrivanek, P. Holec, J. Beran, J. Valtera and M. Bilek, *Sci. Rep.*, 2024, **14**, 24012–24025.
11 A. Stanishevsky, *Macromol. Rapid Commun.*, 2025, 2400907.
12 L. Zhu, B. Zaarour, L. Zhu and X. Jin, *Mater. Res. Express*, 2019, **6**, 125001.
13 W. J. A. Homer, M. Lisnenko, S. Hauzerova, B. Heczkova, A. C. Gardner, E. K. Kostakova, P. D. Topham, V. Jencova and E. Theodosiou, *Polymers*, 2024, **16**, 2079–2097.
14 M. A. Shahid, A. Ali, M. N. Uddin, S. Miah, S. M. Islam, M. Mohebbullah and M. S. I. Jamal, *J. Ind. Text.*, 2021, **51**, 455–469.
15 M. I. Baker, S. P. Walsh, Z. Schwartz and B. D. Boyan, *J. Biomed. Mater. Res., Part B*, 2012, **100**, 1451–1457.
16 C. M. Hassan and N. A. Peppas, *Structure and Applications of Poly (Vinyl Alcohol) Hydrogels Produced by Conventional Crosslinking or by Freezing/thawing Methods in Biopolymers PVA Hydrogels, Anionic Polymerisation Nanocomposites*, Springer, Berlin, Heidelberg, 2000, pp. 37–65.
17 M. L. Hallensleben, R. Fuss and F. Mummy, Polyvinyl Compounds, Others, in *Ullmann's Encyclopedia of Industrial Chemistry*, 2015.
18 B. Golba, O. I. Kalaoglu-Altan, R. Sanyal and A. Sanyal, *ACS Appl. Polym. Mater.*, 2022, **4**, 1–17.
19 E. A. Kamoun, X. Chen, M. S. M. Eldin and E. R. S. Kenawy, *Arab. J. Chem.*, 2015, **8**, 1–14.

20 B. Zaarour, L. Zhu and X. Jin, *ChemistrySelect*, 2020, **5**, 1335–1348.
21 J. S. Stephens, D. B. Chase and J. F. Rabolt, *Macromolecules*, 2004, **37**(3), 877–881.
22 J.-S. Kim and D. S. Lee, *Polym. J.*, 2000, **32**, 616–618.
23 J. Lu, A. Jerschow and D. E. Korenchan, *J. Magn. Reson.*, 2023, **354**, 107529–107536.
24 G. N. Manjunatha Reddy and S. Caldarelli, *Chem. Commun.*, 2011, **47**, 4297–4299.
25 N. Esturau and J. F. Espinosa, *J. Org. Chem.*, 2006, **71**, 4103–4110.
26 J. A. Aguilar, M. Nilsson, G. Bodenhausen and G. A. Morris, *Chem. Commun.*, 2012, **48**, 811–813.
27 P. Moutzouri, P. Kiraly, A. R. Phillips, S. R. Coombes, M. Nilsson and G. A. Morris, *Anal. Chem.*, 2017, **89**, 11898–11901.
28 P. Moutzouri, P. Kiraly, A. R. Phillips, S. R. Coombes, M. Nilsson and G. A. Morris, *Chem. Commun.*, 2017, **53**, 123–125.
29 K. Zangger, *Prog. Nucl. Magn. Reson. Spectrosc.*, 2015, **86**, 1–20.
30 L. Castañar and T. Parella, *Magn. Reson. Chem.*, 2015, **53**, 399–426.
31 K. Zangger and H. Sterk, *J. Magn. Reson.*, 1997, **124**, 486–489.
32 R. Freeman, *Prog. Nucl. Magn. Reson. Spectrosc.*, 1998, **32**, 59–106.
33 M. Foroozandeh, R. W. Adams, N. J. Meharry, D. Jeannerat, M. Nilsson and G. A. Morris, *Angew. Chem., Int. Ed.*, 2014, **53**, 6990–6992.
34 M. Foroozandeh, G. A. Morris and M. Nilsson, *Chem. – Eur. J.*, 2018, **24**, 13988–14000.
35 P. K. N. Kern, M. P. Plesniak, M. Nilsson, D. J. Procter, G. A. Morris and R. W. Adams, *Angew. Chem., Int. Ed.*, 2021, **60**, 666–669.
36 P. T. Robinson, T. N. Pham and D. Uhrín, *J. Magn. Reson.*, 2004, **170**, 97–103.
37 P. Kiraly, M. Nilsson, G. A. Morris and R. W. Adams, *Chem. Commun.*, 2021, **57**, 2368–2371.
38 L. Kocis, P. Pokorny, D. Lukas, P. Mikes, J. Chvojka, E. Kostakova, J. Beran, M. Bilek, J. Valtera, E. Amler, M. Buzgo and A. Mickova, Method for Production of Polymeric Nanofibers by Spinning of Solution or Melt of Polymer in Electric Field, and a Linear Formation from Polymeric Nanofibers Prepared by This Method, *EP Pat.*, EU2931951B1, 2019.
39 B. Ancian, I. Bourgeois, J. E. Dauphi and A. A. Shaw, *J. Magn. Reson.*, 1997, **125**, 348–354.
40 A. Jerschow and N. Müller, *J. Magn. Reson.*, 1997, **125**, 372–375.
41 M. Nilsson, *J. Magn. Reson.*, 2009, **200**, 296–302.
42 M. Foroozandeh, R. W. Adams, N. J. Meharry, D. Jeannerat, M. Nilsson and G. A. Morris, *Angew. Chem., Int. Ed.*, 2014, **53**, 6990–6992.
43 B. Dagès, J. Fabian, D. Polakova, M. Rysova, P. D. Topham, J.-B. Souppez, M. P. Hanga and E. Theodosiou, *Food Bioprod. Process.*, 2025, **149**, 118–129.
44 B. Díez, W. J. A. Homer, L. J. Leslie, G. Kyriakou, R. Rosal, P. D. Topham and E. Theodosiou, *J. Chem. Technol. Biotechnol.*, 2022, **97**, 620–632.
45 C. Oliveira, D. Sousa, J. A. Teixeira, P. Ferreira-Santos and C. M. Botelho, *Front. Bioeng. Biotechnol.*, 2023, **11**, 1136077.
46 M. A. Teixeira, M. T. P. Amorim and H. P. Felgueiras, *Polymers*, 2020, **12**, 7–39.
47 J. Shin, Y. Kim, Y. M. Lim and Y. C. Nho, *J. Appl. Polym. Sci.*, 2008, **107**, 3179–3183.
48 P. Ginestra, E. Ceretti and A. Fiorentino, *Proced. CIRP*, 2016, **49**, 8–13.
49 K. C. Castro, M. G. N. Campos, L. Helena and I. Mei, *Int. J. Biol. Macromol.*, 2021, **173**, 251–266.
50 R. Evans, A. Hernandez-Cid, G. Dal Poggetto, A. Vesty, S. Haiber and G. A. Morris, *RSC Adv.*, 2017, **7**, 449–452.

